A Novel ε-Cleavage within the Transmembrane Domain of the Alzheimer Amyloid Precursor Protein Demonstrates Homology with Notch Processing†

Andreas Weidemann,‡ Simone Eggert,‡ Friedrich B. M. Reinhard,‡ Markus Vogel,‡ Krzysztof Paliga,§ Gottfried Baier,|| Colin L. Masters,⊥ Konrad Beyreuther,‡ and Geneviève Evin*,⊥

Zentrum für Molekulare Biologie Heidelberg, INF 282, 69120 Heidelberg, Germany, MPI for Endocrinology, Hannover, Germany, Molecular Biology and Human Genetics, University of Innsbruck, Innsbruck, Austria, and Department of Pathology, The University of Melbourne, Parkville, Victoria 3052, Australia

Received September 24, 2001; Revised Manuscript Received December 5, 2001

ABSTRACT: Proteolytic processing of the transmembrane domain of the amyloid precursor protein (APP) is a key component of Alzheimer's disease pathogenesis. Using C-terminally tagged APP derivatives, we have identified by amino-terminal sequencing a novel cleavage site of APP, at Leu-49, distal to the γ-secretase site. This was termed ε-cleavage. Brefeldin A treatment and pulse−chase experiments indicate that this cleavage occurs late in the secretory pathway. The level of ε-cleavage is decreased by expression of presenilin-1 mutants known to impair Aβ formation, and it is sensitive to the γ-secretase inhibitors MDL28170 and L-685,458. Remarkably, it shares similarities with site 3 cleavage of Notch-1: membrane topology, cleavage before a valine, dependence on presenilins, and inhibition profile.

The proteolytic processing of the amyloid precursor protein [APP[1] (*1*)] is of central interest to Alzheimer's disease research. One of the resulting cleavage products, the β-amyloid fragment (Aβ), is deposited in the brain of affected individuals as extracellular plaques and congophilic angiopathy. Two major Aβ species are found in these amyloid deposits which differ by the length of their C-terminus, comprising either 40 or 42/43 residues. The longer forms of Aβ are more prone to aggregation and constitute the seeds for senile plaque formation (*2*). The intriguing relationship between Alzheimer's disease and Aβ formation is corroborated by the finding that Aβ formation is affected in some familial forms of the disease caused by autosomal dominant mutations in the gene for APP. These mutations induce either an increased overall level of secretion of Aβ or an increased level of secretion of the longer form $Aβ_{42}$ relative to the shorter 40-amino acid peptide (reviewed in ref *3*). APP is a member of a gene family of homologous integral membrane proteins (*4*−*6*) and undergoes extensive post-translational modifications. After synthesis as a type 1 transmembrane protein, APP matures through the secretory pathway and becomes N- and O-glycosylated, sulfated, and phosphorylated. Additionally, it can be proteolytically processed by a set of proteases; in the major secretory pathway, some of the APP molecules are cleaved by α-secretase within the Aβ sequence, resulting in the release of the APP ectodomain into the extracellular space (*7*). In the alternative, amyloidogenic pathway, a fraction of the APP is processed by β-secretase which leads to secretion of a slightly shorter ectodomain and release, simultaneously, of the N-terminus of the Aβ peptide (*8*−*11*). The membrane-bound proteolytic fragments generated by α- and β-secretases can be further converted by γ-secretase cleavage within the transmembrane domain to form Aβ (∼4 kDa) and p3 (a truncated form of Aβ, ∼3 kDa), both of these peptides ending at either residue 40 or 42 of the Aβ sequence (reviewed in ref *3*). Additionally, under apoptotic conditions, APP is proteolytically converted within its cytosolic domain by caspases (*12*−*15*).

Mutations that are the causes of the majority of cases of early onset FAD that occur before 60 years of age have been identified in the genes encoding presenilin-1 (PS1) and presenilin-2 (PS2) (*16*−*18*). These missense mutations were also found to alter APP processing in a pathological manner by increasing the relative concentration of Aβ ending at residue 42, linking again amyloid formation to Alzheimer's disease (*19*−*23*). The mechanisms by which mutations in the presenilin genes cause an increased level of formation of $Aβ_{42}$ have not been fully resolved yet. These may include some indirect effects, such as activation of the corresponding protease or alteration of vesicular trafficking and, thereby, of APP intracellular transport, or more direct effects, such

† This study was supported by grants from the Alzheimer Forschung Initiative (to A.W.) and from the Deutsche Forschungsgemeinschaft through SFB 488, the Land Baden-Würtemberg, the Metropolitan Life Foundation, the Fond der Chemischen Industrie of Germany, the Erna-Struckmann-Foundation (to K.B.), and the National Health and Medical Research Council of Australia (to C.L.M. and G.E.).

* To whom correspondence should be addressed: Department of Pathology, The University of Melbourne, Parkville, Victoria 3010, Australia. Telephone: +61 3 8344 5867. Fax: +61 3 8344 4004. E-mail: gmevin@unimelb.edu.au.

‡ Zentrum für Molekulare Biologie Heidelberg.

§ MPI for Endocrinology, Hannover.

|| University of Innsbruck.

⊥ The University of Melbourne.

[1] Abbreviations: AD, Alzheimer's disease; APP, amyloid precursor protein; Aβ, amyloid Aβ protein; CTF, C-terminal fragment; ECL, enhanced chemiluminescence; FAD, familial Alzheimer's disease; IgG, immunoglobulin; mAb, monoclonal antibody; PAGE, polyacrylamide gel electrophoresis; PS1, presenilin-1; PS2, presenilin-2; SDS, sodium dodecyl sulfate; SPA4CT, fragment of APP extending from the N-terminus of Aβ to the APP C-terminus and expressed with a signal sequence; SREBP, sterol regulatory element-binding protein; TGN, trans-Golgi network.

10.1021/bi015794o CCC: $22.00
Published on Web 01/30/2002

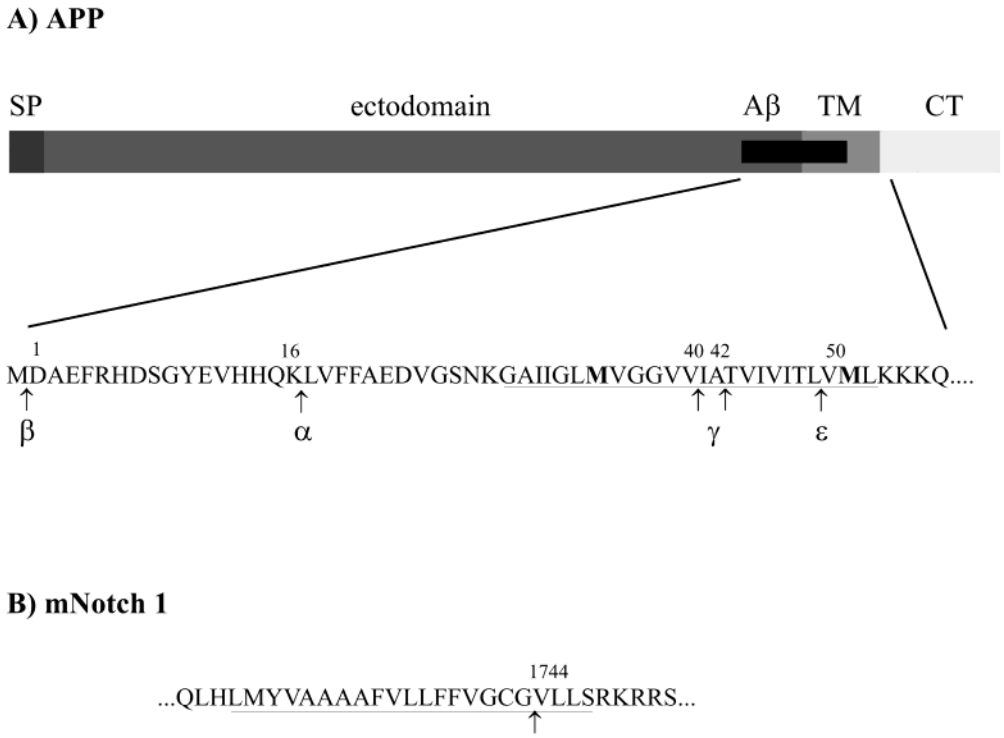

FIGURE 1: Comparison of APP and mNotch-1 cleavage sites within their transmembrane domain. (A) Schematic representation of APP and its transmembrane domain. The large extracellular domain of APP is followed by the Aβ sequence (black bar), the transmembrane domain (TM), and the cytoplasmic domain (CT). The α-, β-, γ-, and ε-cleavage sites are indicated. The predicted transmembrane domain (TM) of APP is underlined. SP, signal peptide. (B) Transmembrane domain of mNotch-1. Like APP, Notch resembles a type I integral membrane protein. Proteolytic processing of Notch includes constitutive cleavage at site 1 and site 2 close to the transmembrane domain. After ligand binding, Notch becomes further processed by cleavage at site 3, before V1744 at the cytosolic site of its transmembrane domain (underlined).

as hampering APP−PS interaction (*24*−*27*) or affecting PS hypothetical γ-secretase activity. Presenilins also interact with another transmembrane protein, Notch-1 (*28*), which, like APP, undergoes proteolytic cleavage within its transmembrane domain by a γ-secretase-like activity that is dependent on PS1 expression (*29*, *30*). The direct interactions between PS and APP and between PS and Notch would be consistent with PS either being cofactors for γ-secretase or being themselves γ-secretase activities (*31*).

Although the exact mechanism by which the C-terminus of Aβ is released by γ-secretase is not fully understood, it is commonly assumed that it involves a single endoproteolytic cleavage within the APP transmembrane to produce either Aβ40 or Aβ42 (*32*). If this were the case, the β-secretase C-terminal fragment, βCTF, comprising the last 99 residues of APP would be converted into Aβ, and a fragment of residues 57−59 (here termed γCTF) that includes part of the transmembrane domain and the entire cytosolic domain (see Figure 1). Similarly, the α-cleaved fragment (αCTF) would be converted into p3 and the same γCTF. However, γCTF has never been clearly identified, and there is no N-terminal sequence data available so far to provide the unambiguous proof that Aβ is produced directly from βCTF by a single endoproteolytic cleavage. Therefore, one cannot exclude the possibility that an intermediate cleavage occurring distal to the γ-cleavage site and followed by γ-cleavage itself, or by multiple exoprotease cuts, may contribute to the formation of Aβ_{40} and Aβ_{42} (*33*, *34*). In an attempt to clarify this question, we developed a method for allowing detection of C-terminal fragments derived from APP processing within its transmembrane domain by stabilizing the APP cytosolic domain as a chimeric fusion protein. With this method, we have isolated a new soluble APP C-terminal fragment. N-terminal radiosequencing revealed this was generated by proteolysis distal to the γ-cleavage site between Leu-49 and Val-50 (numbered relative to the Aβ sequence) and homologous to Notch site 3 cleavage. To follow the nomenclature on APP cleavages that already includes α-, β-, γ-, (reviewed in ref *3*) and δ-cleavage (*35*), this novel cleavage site was termed the ε-cleavage site. Further analysis has revealed that ε-cleavage occurs late in the secretory pathway and is sensitive to γ-secretase inhibitors. Like γ-secretase and Notch site 3 cleavages, APP ε-cleavage is dependent on PS1 as demonstrated by experiments in the presence of functionally inactive PS1 mutants.

EXPERIMENTAL PROCEDURES

DNA Constructs. For generating the 2z-tagged APP derivatives, 2z cDNA was amplified by PCR using pQE60-2z as a template (a kind gift from D. Görlich, Heidelberg, Germany), a sense primer encoding a *Xho*I restriction site and a thrombin (LVPR↓GS) cleavage site (5′-CCCCT-CGAGCTGGTTCCGCGTGGATCGAAAGAGGAGAAA-TTAACC-3′), and an antisense primer encoding a stop codon and a *Cla*I restriction site. The resulting PCR fragment was subcloned into pBluescript SK+ (Stratagene) by using the *Xho*I and *Cla*I restriction sites. SPA4CT encoding cDNA was amplified by PCR with an antisense primer encoding a *Sal*I site (5′-GGCTGAGTCGACGTTCTGCATCTGCT-CAAAG-3′) and subcloned into pBluescript SK+. The *Sal*I site was ligated with the *Xho*I site of the 2z subclone, resulting in SPA4CT-2z. An internal *Eco*RI site within the open reading frame of SPA4CT-2z was used to create full-

length APP-2z encoding 833 amino acids. For expression of γCTF-2z, a methionine start codon was engineered at position V_{41}. For construction of εCTF-2z, the internally encoded M_{51} was preceded by a consensus sequence for the initiation of translation (CCACC), and a *Kpn*I cloning site. Both cDNAs were cloned into pBluescript SK+ and used for in vitro translation experiments. γCTF-2z was additionally cloned into pCEP4. SPA4CT-2z derivatives carrying the mutations within the transmembrane domain (T43P, V50K, V50L, and L49P) were produced by PCR using SPA4CT-2z as a template. After sequencing of the coding regions that were amplified by PCR had been carried out, all APP-derived constructs were cloned into the eukaryotic expression vector pCEP4 (Invitrogen). Cloning of wt-PS1 cDNA has been described previously (*36*, *37*). Mutants PS1-D253A and PS1-D253A/D381A were created by PCR-based mutagenesis. After sequencing had been carried out, wild-type and mutant PS1 cDNAs were cloned into pcDNA3.1-neo (Invitrogen). Preparation of rabbit polyclonal anti-APP antiserum has been described previously (*7*).

Immunoblotting and Radiosequencing. Lysis of cells and immunoprecipitation of APP were performed as described previously (*7*). 2z-tagged proteins were immunoprecipitated using human IgG immobilized to Sepharose (Amersham). For thrombin cleavage, Sepharose beads were incubated in 10 mM Tris-HCl (pH 7.5) with 0.1 unit of thrombin for 1.5 h at 37 °C. Membrane fractionation was performed by hypotonic swelling of the cells in 10 mM Tris-HCl (pH 7.5), 1 mM EDTA, and 1 mM EGTA for 15 min on ice, followed by repeated passage through a 27 gauge needle. Centrifugation for 5 min at 1200 rpm yielded a postnuclear supernatant which was centrifuged for 30 min at 100000*g*. The pellet, containing a crude membrane fraction and mitochondria, and the supernatant, containing cytosolic proteins, were analyzed separately.

For the analysis of CTFs, samples were denatured in sample buffer in the absence of reducing agents and electrophoresed either on 15% Tris-Glycine gels or on 10−16.5% Tris-Tricine gels. After Western blotting, samples were immunodetected by incubation with nonspecific rabbit antiserum as the primary antibody followed by anti-rabbit serum coupled to horseradish peroxidase and ECL development. For radiosequencing of metabolically labeled proteins, APP CTFs were immunoprecipitated, electrophoresed, and transferred to polypropylene membranes. After autoradiography, individual strips corresponding to the visualized bands were excised and subjected to automated Edman degradation (Applied Biosystems). Fractions were collected at each cycle, and the radioactivity was quantified by scintillation counting.

Cell Culture. For selection of stable cell lines, cells were transfected with the corresponding plasmid by $CaPO_4$ coprecipitation following with selection in medium containing 400 μg/mL hygromycin. Cells were treated with the following compounds: 10 μg/mL Brefeldin A (Biomol), 100 μM MDL28170, and L-685,458 as indicated [provided by Merck Sharp & Dohme (*38*, *39*)].

RESULTS

Since the C-terminal product of γ-secretase cleavage has never been characterized, we reasoned that this rather small protein fragment of 57−59 residues might be difficult to detect because of a rapid cellular turnover. To increase its stability, a tag encoding two z-domains cloned in tandem was fused to the APP C-terminus. The z-domain corresponds to the region of protein A that mediates binding to immunoglobulins (∼about 70 residues); thus, the presence of this tag allowed the direct precipitation of APP and its C-terminal fragments with immunoglobulin-coated Sepharose. A thrombin cleavage site was engineered between the APP coding region and the 2z tag to allow removal of the tag.

Expression of APP695-2z was analyzed in stably transfected, human neuroblastoma SH-SY5Y cells after metabolic labeling with [^{35}S]methionine and immunoprecipitation with IgG-Sepharose. For comparison, SH-SY5Y cells expressing wild-type APP695 were also analyzed by immunoprecipitation with anti-APP polyclonal antiserum. Full-length APP695 was detected in cell lysates as a doublet of ∼100−105 kDa that corresponds to immature, N-glycosylated species (Figure 2A, lane 1). Additional signals of 115−125 kDa were observed that represent post-translationally modified APP derived by successive transport of APP through the Golgi apparatus where it undergoes O-glycosylation, sulfation, and phosphorylation (*7*). The chimeric APP695-2z migrated as two bands with apparent molecular masses of 120 and 140 kDa corresponding to the immature and mature forms, respectively (Figure 2A, lane 2). These molecular masses are consistent with the addition of two z-tags (14 kDa) to APP. The 140 kDa band, corresponding to mature APP-2z, appears to be relatively more intense than the 115−125 kDa signal observed for full-length wild-type APP. The reason may be that the bands are more condensed due to the lower resolution of the higher-molecular mass proteins, and/or because the presence of the tags confers greater stability to mature APP. The observed signals were absent from nontransfected cells (Figure 2A, lane 3). To check that the intracellular transport of APP695-2z was not affected by the 2z tag, the proteolytic conversion of membrane-bound APP by α-secretase was analyzed by immunoprecipitation of soluble APP695 from the cell-conditioned medium. The relative amount of secreted versus intracellular APP695 species was very similar for both APP695 and APP695-2z cell lines, indicating that proteolytic processing by α-secretase was not altered by the 2z tag (lanes 4 and 5). Immunoprecipitation of Aβ and p3 from SH-SY5Y-conditioned medium using antibodies that recognize either the Aβ N-terminal region [W02, Figure 2B, lanes 1−3 (*39*)] or the Aβ and p3 C-terminus produced by γ-secretase conversion at position 40 [G2−10, Figure 2B, lanes 4−6 (*40*)] showed similar results for both cell lines. These results demonstrate that APP processing by both β- and γ-secretases was not hampered by the C-terminal fusion. To investigate the carboxy-terminal processing of APP by secretases, cellular immunoprecipitates were analyzed on high-percentage acrylamide gels (Figure 2C). In cell lysates derived from APP695-2z-transfected SH-SY5Y and COS7 cells, two major bands of ∼27 and ∼23 kDa were detected (Figure 2C, lanes 1 and 4). As deduced from their relative molecular mass, those fragments could represent the carboxy-terminal fragments derived from cleavages by α- and γ-secretases, respectively. In the neuronal SH-SY5Y cells (Figure 2C, lane 1), two prominent additional bands were detected, which reflect proteolytic processing of APP by β-secretase. The upper band has the expected size for βCTF (lane 1) as

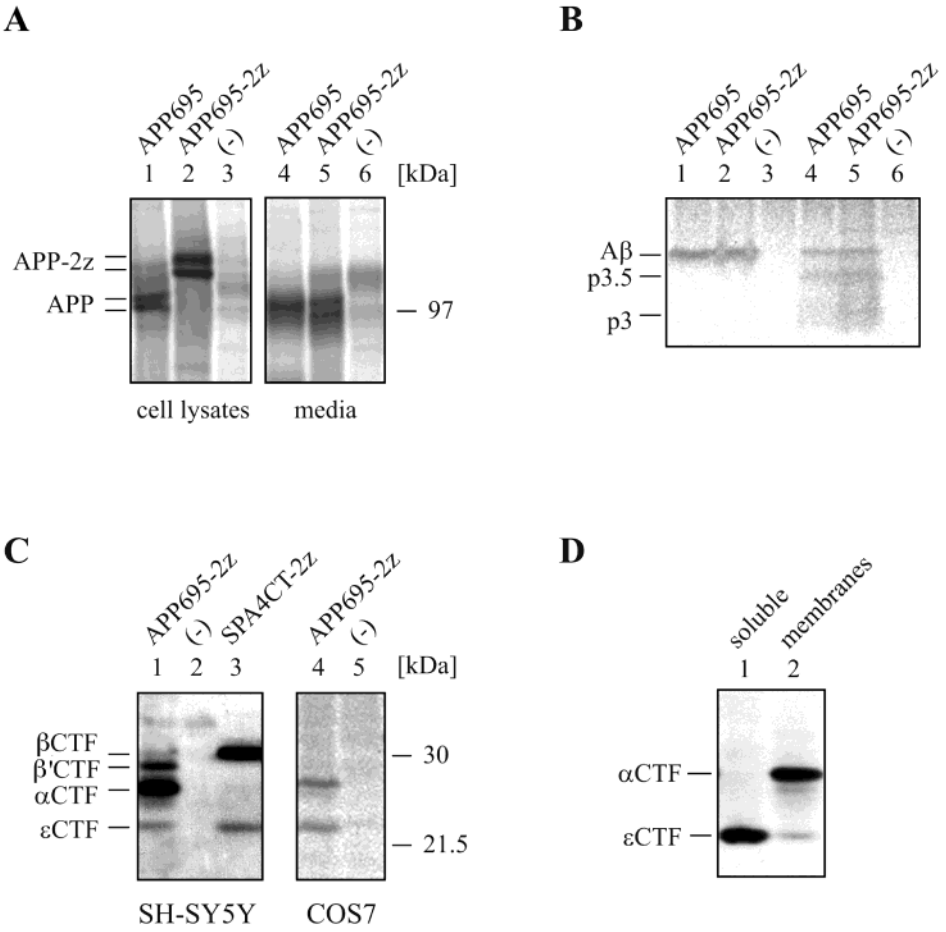

FIGURE 2: Expression of APP695 as a 2z-tagged chimeric protein and identification of C-terminal fragments. (A) Detection of cellular and secretory APP695 and APP695-2z in SH-SY5Y cells. Cellular (lanes 1−3) and secretory APP (lanes 4−6) was analyzed from stably transfected SH-SY5Y cells expressing either APP695 (lanes 1 and 4) or APP695-2z (lanes 2 and 5) or empty vector (lanes 3 and 6). Cells were labeled for 6 h with [^{35}S]methionine followed by immunoprecipitation with anti-APP polyclonal rabbit serum and protein A-Sepharose. (B) Formation of Aβ and p3 is similar for SH-SY5Y cells expressing APP695 or APP695-2z. For detection of Aβ and p3, the conditioned media of [^{35}S]methionine-labeled cells were immunoprecipitated either with the monoclonal antibody W02, directed against the N-terminal part of Aβ (lanes 1−3), or with G2−10, recognizing Aβ and p3 fragments that end with V_{40} (lanes 4−6). (C) Analysis of APP C-terminal fragments. C-terminal fragments were analyzed from SH-SY5Y cell lysates (lanes 1−3) and COS7 cells (lanes 4 and 5) stably overexpressing APP695-2z (lanes 1 and 4) or SPA4CT-2z (lane 3) or from control cells (lanes 2 and 5). In APP695-2z-expressing cells (lanes 1 and 4), two major bands are detected at 27 and 23 kDa, representing α- and εCTF, respectively. In SH-SY5Y cells (lane 1), two additional bands are detected, the upper one with the expected size for βCTF and the same electrophoretic mobility as the βCTF reference expressed in SPA4CT-2z-transfected cells (lane 3). Cell lysates were subjected to immunoprecipitation with IgG-Sepharose, followed by immunoblotting with nonspecific rabbit antiserum and ECL. (D) Detection of εCTF as a soluble peptide. Soluble (lane 1) and membrane-associated proteins (lane 2) from APP695-2z-expressing COS7 cells were separated by ultracentrifugation followed by immunoblotting with nonspecific rabbit antiserum and ECL.

compared with SPA4CT-2z-expressing cells (lane 3). The lower band was labeled β'CTF as this is likely to represent the alternative β-secretase product that leads to the formation of p3.5 (Figure 2B, lanes 4 and 5). The 23 kDa band was also produced in cells expressing SPA4CT-2z (Figure 2C, lane 3), a construct that mimics the APP β-secretase C-terminal product, βCTF.

To determine the membrane association of the APP CTFs, membrane-bound and soluble proteins were separated by ultracentrifugation of the cell lysates. The 27 kDa CTF was identified in the 100000*g* pellet, suggesting it is a membrane-associated protein (Figure 2D, lane 2), whereas the 23 kDa fragment was predominantly found in the soluble fraction (100000*g* supernatant), as expected for a product released in the cytosol (Figure 2D, lane 1).

Identification of the APP ε-Cleavage Site. Radiosequencing of the [^{35}S]methionine-labeled 27 kDa band (data not shown) confirmed its identity as the α-secretase-derived fragment and showed the presence of a minor cleavage product starting at residue G_{25} which most likely corresponds to the faint 26 kDa signal observed in lane 1 of Figure 2C. The 23 kDa fragment was expected to result from γ-secretase cleavage, and sequencing was anticipated to yield radioactive peaks at cycle 11 (cleavage after V_{40}) and/or at cycle 9 (cleavage after A_{42}). Unexpectedly, a single peak was observed at cycle 2, whenever the fragment was derived from COS7 or from SH-SY5Y cells, thereby identifying its N-terminus as V_{50} (Figure 3A; indicated in Figure 1A). Indeed, the methionine residues in the C-terminal region of APP are located at positions 631 (Aβ position 35), 647 (Aβ position 51), 677, and 693. If the radioactive methionine that was detected was residue 631, a second peak should be observed at cycle 17, and if it was M_{677}, a second peak would appear at cycle 18. As no other peak of radioactivity was observed within 25 Edman degradation cycles, the radioactive peak detected at cycle 2 was attributed to M_{647}

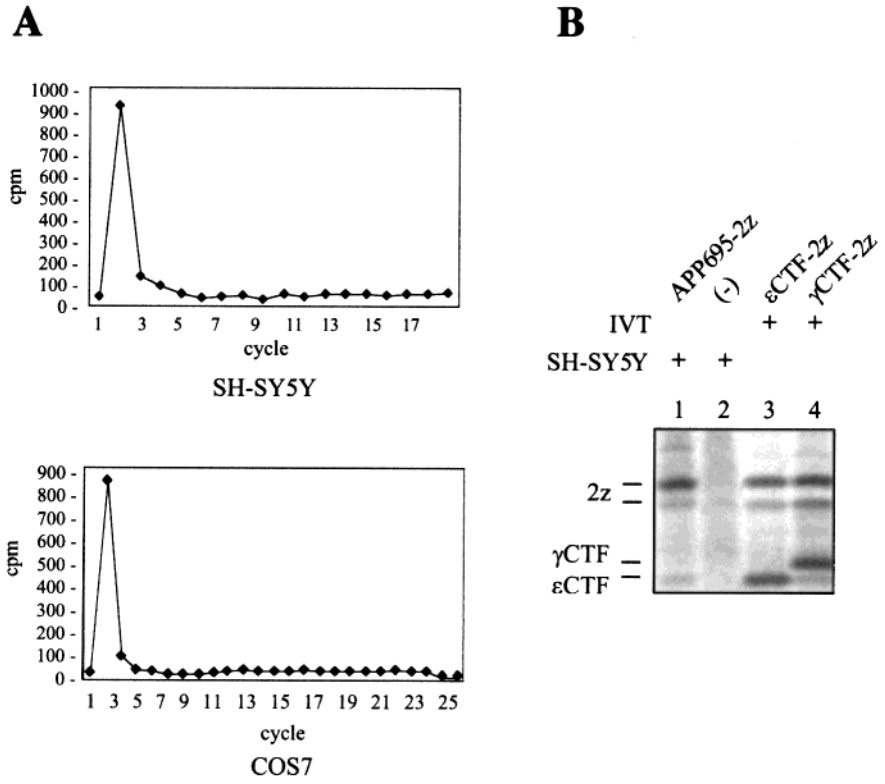

FIGURE 3: Identification of the APP ε-cleavage site. (A) Radiosequencing of the 23 kDa band derived from SH-SY5Y and COS7 cells. A single radioactive peak was observed in the second Edman degradation cycle of the 23 kDa product. No signals were detected in cycles 9 and 11, which would be expected for proteolytic fragments derived by γ-secretase cleavage releasing Aβ40 and Aβ42, respectively. SH-SY5Y and COS7 cells stably expressing APP695-2z were metabolically labeled with [^{35}S]methionine, followed by immunoprecipitation with IgG-Sepharose. Bound immunocomplexes were separated by PAGE and blotted on PVDF membranes. After autoradiography, the 23 kDa band was excised and subjected to Edman degradation. The fractions of each cycle were collected, and the amount of radioactivity was determined by scintillation counting. (B) Separation of εCTF and γCTF by SDS−PAGE. εCTF derived from SH-SY5Y cells expressing APP695-2z (lane 1) displays the same mobility on gels as in vitro-translated εCTF (lane 3) but not the same as γCTF (lane 4; the additional εCTF band in this lane is derived by alternative initiation of translation at the internal M_{51} codon). For further identification of the cellular fragment as εCTF, two mutants were constructed in which either a methionine start codon was introduced at position V_{41} (γCTF-2z) or the internally encoded M_{51} was used for initiation of translation (εCTF-2z). Both proteins were translated in vitro using rabbit reticulocyte lysates in the presence of [^{35}S]methionine (IVT, lanes 3 and 4). In parallel, cellular fragments were immunopurified from [^{35}S]methionine-labeled APP695-2z-expressing SH-SY5Y cells. Bound complexes were digested with thrombin to release the 2z tag (upper bands), resulting in γCTF and εCTF (lower bands) followed by separation on Tris-Tricine gels.

(Aβ residue M_{51}). Thus, the 23 kDa band did not represent the C-terminal fragment expected to be generated by γ-secretase but a fragment resulting from cleavage at a new site, between Leu_{49} and Val_{50}, that we termed the "ε-cleavage site".

To prove further that the radioactive methionine detected at cycle 2 had been correctly assigned to M_{51}, the electrophoretic mobility of cellular APP CTFs was compared to that of two standard constructs. In the first construct, a methionine start codon was introduced at position V_{41} (γCTF-2z), and in the second, the internally encoded M_{51} was used for initiation of translation (εCTF-2z). Both proteins were translated in vitro using rabbit reticulocyte lysates. γCTF-2z was also stably expressed in SH-SY5Y cells and compared with the CTFs derived from APP695-2z immunoprecipitates. Initially, no difference was detected in the apparent molecular masses of γCTF-2z and εCTF-2z, both fragments migrating with the same electrophoretic mobility at 23 kDa (data not shown). However, when the 2z tag was removed by digestion with thrombin prior to gel electrophoresis, much smaller peptides were obtained that could be separated on Tris-Tricine gels according to their relative molecular masses. The new fragment derived from the SH-SY5Y cells expressing APP695-2z (Figure 3B, lane 1) migrated with the same mobility as the εCTF standard (Figure 3B, lane 3), whereas γCTF migrated more slowly (Figure 3B, lane 4). No band was detected in APP695-2z immunoprecipitates that migrated with the apparent molecular mass expected for γCTF, confirming the data from the radiosequencing experiments where no radioactivity was detectable at either cycle 9 or 11 (Figure 3A).

The topology of the APP ε-cleavage resembles that reported for mNotch-1 transmembrane cleavage (*41*); both cleavage sites are located close to the predicted membrane boundary (Figure 1A,B) ,whereas the position of the APP γ-cleavage site suggests proteolysis in the middle of the transmembrane domain (*32*). Additionally, ε-cleavage occurs before a valine residue as observed for mNotch-1 (*41*). To compare ε-cleavage with APP γ-cleavage and with Notch cleavage, several additional experiments were carried out, as outlined below.

APP ε-Cleavage Occurs Late in the Secretory Pathway. Pulse−chase experiments were performed to further characterize the formation and turnover of εCTF. SH-SY5Y cells stably transfected with APP695-2z were pulse labeled for 10 min in the presence of [^{35}S]methionine, and chased for various periods of time (Figure 4A,B). Full-length APP695-2z was already detected at the 0 min chase, whereas αCTF

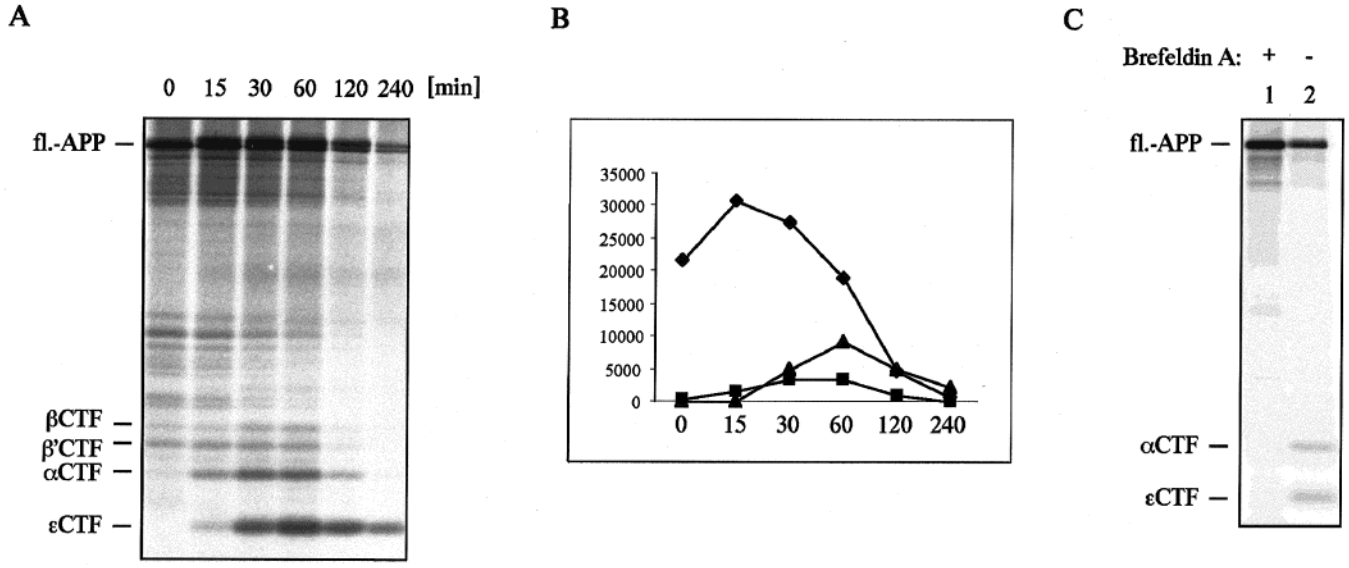

FIGURE 4: ε-Cleavage occurs late in the secretory pathway. (A) Pulse−chase analysis of α- and ε-cleavage. At early chase times of 0 and 15 min, only minor amounts of CTFs are visible, whereas after 30 and 60 min of chasing, α-, β-, and εCTF-2z are detected, as expected for a conversion taking place late in the secretory pathway. SH-SY5Y cells expressing APP695-2z were pulse labeled for 10 min with [^{35}S]methionine followed by chase times as indicated in methionine-enriched media. 2z-encoding proteins were immunoprecipitated with IgG-Sepharose followed by PAGE and phosphorimaging. (B) Densitometric quantitation and graphic representation of the results of the pulse−chase experiment depicted in panel A: (◆) full-length APP, (■) αCTF, and (▲) εCTF. Note that for graphical representation, the values for αCTF and εCTF are depicted after multiplication by a factor of 5. (C) Inhibition of α- and ε-cleavage by Brefeldin A. To block protein transport to the TGN, COS7 cells expressing APP695-2z were labeled with [^{35}S]methionine either in the presence of 10 μg/mL Brefeldin A (lane 1) or in its absence (lane 2) for 3 h followed by immunoprecipitation with IgG-Sepharose and PAGE.

appeared only after 15 min to reach maximal concentrations after 30−60 min of chasing. This result is in agreement with previous reports demonstrating that APP conversion by α-secretase takes place late in the secretory pathway, within the TGN, secretory vesicles, and at the plasma membrane (*42*, *43*). εCTF also appeared after 15 min, and reached a maximal concentration after 120−240 min of chasing, suggesting it is produced in the same compartments of the secretory pathway as is αCTF, but that it accumulates over a much longer period of time and may thus constitute a cleavage product of αCTF. By treating APP695-2z COS7 cells with Brefeldin A, we confirmed that ε-cleavage occurs late in the secretory pathway, after APP moves through the Golgi. Brefeldin A causes the formation of an ER−Golgi continuum and blocks protein transport to the TGN (*44*) and thereby inhibits the conversion of APP by α-secretase in the consecutive compartments of the secretory pathway. Like α-secretase conversion, ε-cleavage was inhibited in the presence of Brefeldin A (Figure 4C, lane 1), substantiating the suggestion that APP ε-cleavage occurs at the earliest in the TGN.

Protease Inhibitor Profile of APP ε-Cleavage. To further characterize the proteases involved in ε-cleavage, we employed inhibitors reported to inhibit γ-secretase and Notch processing, including MDL28170 which represents a broad spectrum calpain inhibitor (*33*, *44*−*46*) and the potent "γ-secretase inhibitor" L-685,458 (*38*, *39*). Because MDL28170 is cytotoxic upon prolonged treatment, cells were labeled for short periods of time (6 h) in the presence of [^{35}S]-methionine plus 100 μM MDL28170 (Figure 5A, lane 4) or solvent only (DMSO, lane 3). MDL28170 caused accumulation of both αCTF and βCTF as reported by others (*33*, *45*−*47*) and commonly interpreted as inhibition of γ-secretase activity. Remarkably, the extent of formation of εCTF was concomitantly decreased. When more specific γ-secretase inhibitors such as the aspartyl protease inhibitor L-685,458 were employed, the concentration of αCTF and βCTFs increased in a dose-dependent manner (Figure 5B) and paralleled the level of inhibition of Aβ release (Figure 5B, bottom panel), confirming previous reports (*45*, *46*). Concomitantly, the formation of εCTF was inhibited, indicating that this specific inhibitor abolishes both Aβ formation and ε-cleavage of APP and suggesting these two events are linked.

APP ε-Cleavage Is Dependent on Presenilin-1. It has been shown that the conversion of APP C-terminal fragments and the release of Aβ peptide depend on the expression of functional presenilins. To test whether ε-cleavage might also depend on presenilins, we coexpressed APP-2z with either wild-type PS1 or PS1 dominant negative mutants. Indeed, it has been shown that mutating PS1 aspartates 257 and 385 (residues 253 and 381 in our PS1 construct) to alanine results in the accumulation of uncleaved PS1 and disables γ-secretase (*31*). By comparison with cells that overexpress wild-type PS1 (Figure 6A, lane 2), expression of the dominant negative mutants PS1-D253A/D381A and PS1-D253A (lanes 3 and 4, respectively) resulted in an accumulation of αCTF, similar to that reported previously (*31*). Concurrently, the level of formation of the ε-cleaved fragment was decreased, suggesting that ε-cleavage is dependent on the expression of functional PS1.

Analysis of APP ε-Cleavage Site Mutants. Because the ε-cleavage site of APP shares similarities with cleavage site 3 of Notch-1, including membrane topology and cleavage before a valine, we tested whether mutations at the cleavage site would abolish proteolytic conversion as reported for Notch-1 processing. Indeed, single-point mutations of mNotch V_{1744} to K or L have been reported to inhibit the proteolytic conversion and release of the cytosolic fragment NICD (*41*). Analysis of SPA4CT-2z mutants (V50K and V50L) revealed

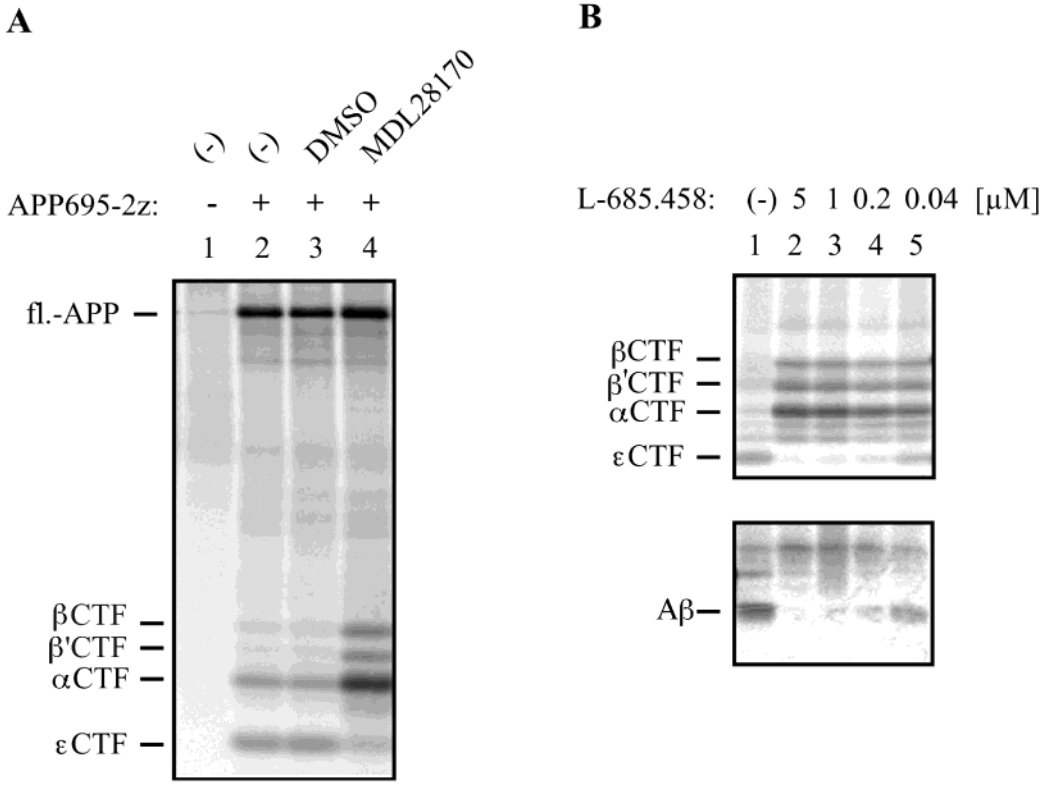

FIGURE 5: Protease inhibitor profile of APP ε-cleavage. Effect of MDL28170 (A) and L-685,458 (B) on ε-cleavage. As compared with controls (lanes 2 and 3), incubation of cells with the calpain inhibitor MDL28170 (lane 4) increases the cellular concentration of β-, β'-, and αCTF, whereas the extent of formation of εCTF is reduced. Similarly, incubation of cells with the more specific γ-secretase inhibitor L-685,458 (B) also caused an accumulation of CTFs concurrent with a decrease in the concentration of εCTF and in the formation of secretory Aβ (B, bottom panel). SH-SY5Y cells were labeled for 6 h with [^{35}S]methionine in the presence of 100 μM MDL28170 in 0.5% DMSO (lane 4), left untreated (lane 2), or incubated in the presence of 0.5% DMSO alone (lane 3). SH-SY5Y cells transfected with the empty vector were used as a control (lane 1). The experiment depicted in B was performed by incubating cells expressing APP695-2z in the presence of L-685,458 and [^{35}S]methionine for 10 h, followed by immunoprecipitation with IgG-Sepharose (top panel) or with monoclonal anti-Aβ antibody W02 (bottom panel).

that neither of these mutations affected ε-cleavage (Figure 7, lanes 2 and 3). Among a series of mutants that we created, two displayed significant alteration of APP transmembrane cleavage. Replacement of threonine 43 or leucine 49 with proline resulted in a decreased level of formation of ε-CTF (Figure 7, lanes 1 and 4). These mutations also caused a high-level reduction of secretory Aβ (data not shown) as reported previously for the T43P mutant (*32*). Because introducing a proline residue within a transmembrane domain would likely perturb the predicted α-helical structure, these mutations may either directly inhibit cleavage, interfere with the binding of cleavage-associated proteins such as nicastrin, or even alter membrane insertion and cellular trafficking of these constructs.

DISCUSSION

The proteases involved in the generation of the Aβ amyloid peptide are potential targets for the development of a therapy for Alzheimer's disease. However, the unusual mechanism, by which one or several γ-secretases cleave APP within its predicted transmembrane domain, is poorly understood. It is commonly assumed that α- and β-cleaved APP fragments are converted by a single γ-secretase cleavage within the transmembrane domain, at either position 40 or 42. To our knowledge, the C-terminal fragment that would result from γ-secretase cleavage and encompass the C-terminal part of the transmembrane domain (starting at residue 41 or 43 relative to the Aβ sequence) and the entire cytoplasmic domain of APP has never been identified. Two recent studies report formation of a γCTF in cell free systems using γ-secretase-enriched preparations (*48*, *49*). The described fragments have the correct electrophoretic mobility to represent γCTF, but no N-terminal sequence data are provided that would confirm their identity. Other studies have proposed that proteolysis of the APP carboxy terminus might be initiated by cytosolic proteases at the very end of the transmembrane domain to release the hydrophobic domain from the membrane and allow subsequent cleavage by more conventional endo- or exoproteases (*50*). To further characterize the conversion of APP within its transmembrane domain, we have expressed APP as a C-terminal fusion protein with a 2z tag to improve the stability of γCTF. We proved that this tag did not interfere with α- and β-secretase cleavages or with Aβ and p3 production (Figure 2). Expression of this chimeric protein allowed detection of a C-terminal fragment produced by endoproteolysis of the APP transmembrane domain. As expected for a cleavage product that lacks a functional transmembrane domain, this was detected as a soluble intracellular species (Figure 2D). N-terminal sequencing of the fragment produced by both SH-SY5Y and COS7 cells revealed a novel cleavage site between L_{49} and V_{50}, close to the C-terminal end of the APP transmembrane domain (Figure 3A). To distinguish this novel cleavage site from the γ-secretase site, it was termed the

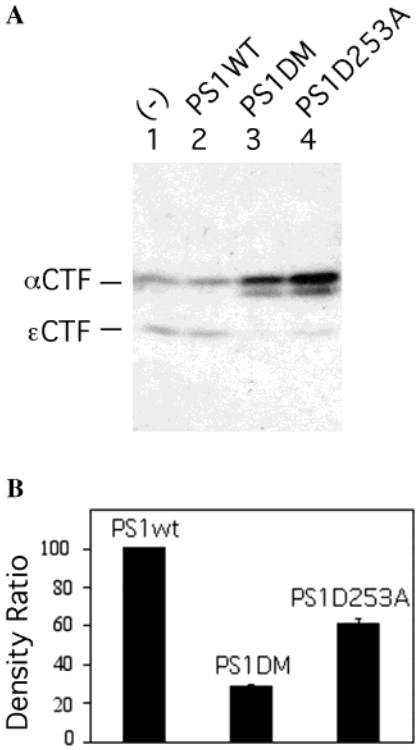

FIGURE 6: ε-Cleavage is dependent on functional PS1. (A) Expression of PS1 D/A mutants increases the cellular concentration of αCTF with a concurrent decrease in the level of εCTF formation. COS7 cells were transiently transfected with two plasmids, one encoding APP695-2z (lanes 1−4) and the second encoding either a nonrelated control plasmid (lane 1), wild-type PS1 (PS1WT; lane 2), PS1-D253A/D381A (PS1DM; lane 3), or PS1-D253A (lane 4). The cells were harvested 24 h after transfection, and the 2z-encoding proteins were immunoprecipitated, followed by SDS−PAGE analysis, immunoblotting, and ECL detection. (B) Comparative quantitative analysis of the εCTF signal in cells transfected with PS1WT and mutants. The ECL films were scanned and the band densities quantitated using NIH Image 1.60 software. The graph represents the average of data obtained from two independent experiments. The expression of PS1 mutants D253A/D381A and D253A caused a reduction of 71 and 29% of the magnitude of the ε-CTF signal, respectively, as compared to PS1WT.

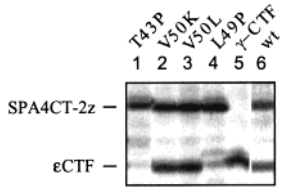

FIGURE 7: Proteolytic processing of SPA4CT derivatives encoding mutations within the predicted transmembrane domain. Mutant SPA4CT-2z derivatives carrying single-point mutations homologous to those that inhibit Notch-1 site 3 cleavage do undergo processing at the ε-site (V50K, lane 2; V50L, lane 3). Introduction of a proline residue at either position 43 (T43P, lane 1) or position 49 (L49P, lane 4) significantly reduced the extent of ε-cleavage. Cells expressing γCTF (lane 5) or wild-type SPA4CT-2z (lane 6) were included for a comparison.

ε-cleavage site. Our result is consistent with a very recent report (*51*) that has characterized, in purified rat brain membrane preparations, APP fragments starting at valine 50, suggesting that native APP is also processed at the ε-cleavage site. In addition, during the preparation of this paper, two other groups published reports that corroborate our results (*52*, *53*).

We have characterized ε-cleavage by showing that it takes place late in the secretory pathway or in the endocytic and/or recycling pathway, it is dependent on active presenilins and can be blocked by inhibitors of Aβ secretion. All these characteristics are shared with γ-secretase activity as deduced from studies of Aβ production. Neither in the radiosequencing experiments nor in the analysis of CTFs by SDS−PAGE were we able to detect a radioactive peak or fragment corresponding to γCTF (Figure 3A,B), although APP-2z was converted by γ-secretase(s) as evidenced by the formation of Aβ and p3 (Figure 2B). In principle, εCTF could be derived from γCTF by the rapid action of a second protease, i.e., in the cell cytosol, and this would explain the difficulty in detecting γCTF and the unexpected finding of an ε-cleavage product. This would also be consistent with the finding that inhibitors of Aβ secretion inhibit the formation of εCTF (Figure 5A,B), as these would act upstream of ε-cleavage. In the same manner, presenilin dominant negative mutants would affect ε-cleavage by interfering with the preceding γ-secretase cleavage (Figure 6A). However, cell transfection with a construct resembling the hypothetical γCTF-2z cleavage product did not reveal production of εCTF (data not shown), arguing against the conversion of γCTF to εCTF.

Alternatively, ε-cleavage may represent an intermediate step in Aβ formation that would precede γ-cleavage, at position 40 or 42. The results of the pulse−chase experiments indicate that εCTF is produced late in the secretory pathway (Figure 4), a finding consistent with the major site of intracellular Aβ production. They also show that αCTF is rapidly turned over while εCTF accumulates, and this is consistent with a precursor−product relationship between αCTF and εCTF. The results of the inhibition studies would also support the idea that ε-cleavage is an intermediate step in Aβ formation. MDL28170, an inhibitor of cysteine proteases and of calpains, was previously reported to block Aβ secretion and to cause accumulation of CTF products of α- and β-secretases (*33*, *45*−*47*), a result confirmed in our study. We found that this compound also inhibits the formation of εCTF, suggesting Aβ and εCTF may represent the products of similar proteolytic activities (Figure 5A). Furthermore, we found that the most potent and specific inhibitor of γ-secretase reported so far, L-685,458 (*38*, *39*), also inhibits εCTF formation (Figure 5B) with concomitant accumulation of α- and βCTF. The effect of L-685,458 on ε-cleavage was observed with inhibitor concentrations as low as 40 nM and paralleled its effect on Aβ secretion, suggesting that both events are directly linked. The dependence of ε-cleavage on active presenilins (Figure 6), demonstrated by using dominant negative mutants, could also be explained if ε-cleavage represented an intermediate step in the γ-secretase pathway. Such PS1 dominant negative mutants have been shown to affect Aβ production and Notch cleavage in a manner similar to PS1 gene knockout (*28*, *31*, *54*, *55*). We may also propose that ε-cleavage likely precedes γ-cleavage on the basis of previous studies. Phenylalanine scanning of the APP transmembrane domain has identified position 50 as being critical for Aβ formation (*32*). Furthermore, mass spectrometry analysis of Aβ species from skeletal muscles has characterized Aβ peptides extended at their C-terminus, up to residue 46 (*56*), suggesting that a first cleavage(s) at a site distal to the γ-secretase site may precede

the γ-cut. Another interpretation of our results would be that γ- and ε-cleavages constitute separate proteolytic events occurring in parallel. Because both cleavages require presenilins and both are sensitive to the same class of inhibitors, these would likely be carried out by similar proteases or by the same proteolytic complex.

ε-Cleavage is the fifth proteolytic cleavage reported so far to require presenilins, after APP γ-secretase, Notch site-3, IRE1 processing, and cleavage of the ErbB-4 receptor tyrosine kinase (*57*) [although the effect on IRE1 is controversial (*58*)]. This would suggest that the same PS1-associated proteolytic activity or proteolytic complex effects these cleavages. Recent data indicate that PS1 is associated in a multimeric high-molecular mass complex containing γ-secretase activity (*59*). This complex may include the PS1 binding partners β-catenin (*60*) and nicastrin (*61*) as well as yet undefined proteins and proteases, and it would constitute a multicatalytic activity resembling the proteasome and termed the "secretasome" (*61*).

APP ε-cleavage shares important similarities with the cleavage of Notch within its transmembrane domain, at site 3 (*62*): dependence on active presenilins, inhibition profile, and membrane topology of the cleavage site. Both APP ε-cleavage and Notch site 3 cleavage occur close to the cytoplasmic face, whereas the APP γ-cleavage site is located in the middle of the transmembrane domain. ε-Cleavage is also reminiscent of the cleavage of another transmembrane protein, the sterol-binding regulatory element protein (SREBP) that is processed by a novel type of membrane metalloprotease that cleaves three residues from the predicted membrane boundary (reviewed in ref *62*). In each of these cases, the APP ε-site, the Notch site-3, and SREBP, proteolysis of the transmembrane domain does not take place in the depths of the hydrophobic membrane environment but at a homologous site close to the membrane−cytoplasm interface. For both APP ε-cleavage and Notch site 3 cleavage, proteolysis occurs before a valine residue (Figure 1), supporting further the idea that the same protease activity is involved in both cleavages. However, site-directed mutagenesis of the ε-cleavage site did not indicate sequence specificity, except when valine 49 was substituted with the α-helix breaker proline (Figure 7). In contrast, Notch cleavage is altered by substituting the cleavage site valine 1744 with Leu or Lys (*41*). This difference may be attributed to interactions with different binding or presenting partners rather than enzyme cleavage specificity. To support the suggestion that Notch site 3 cleavage is due to the same protease as that cleaving APP at the ε-site, we have shown that ε-cleavage is blocked by the aspartyl protease inhibitor L-685,458, a potent, specific inhibitor of Aβ formation and of Notch signaling (*63*) (Figure 5B). Whether L-685,458 inhibits both γ- and ε-cuts or if it exerts its effect on Aβ production by blocking cleavage at the ε-site rather than at the γ-site will need to be clarified. If it does interfere with cleavage at the γ-site, one may question whether Notch transmembrane processing also involves an intermediate cleavage step, in the middle of the transmembrane domain and homologous to the γ-secretase cleavage of APP.

Notch site 3 cleavage serves to release the soluble cytosolic fragment NICD that acts as a transcription factor. Recent studies have shown that the cytosolic domain of APP regulates diffusion of the protein adapter Fe65 to the nucleus (*64*, *65*) and may be part of a signaling system. ε-Cleavage that results in release of the cytosolic domain of APP would thus play an important role in this mechanism. Our preliminary data indicate that εCTF is present in cellular nuclear fractions. Further studies will be required to clarify the function of this cleavage.

In conclusion, our finding of a novel cleavage within the transmembrane domain of APP opens new questions concerning the proteolytic mechanisms that produce Aβ and those that process the Notch transmembrane domain. A recent study demonstrates it is possible to inhibit Aβ production without affecting Notch cleavage (*66*). If Notch site 3 protease and ε-secretase happen to be the same protease but distinct from γ-secretase, it might be possible to manipulate pharmacologically Aβ production with γ-secretase inhibitors without interfering with Notch signaling.

ACKNOWLEDGMENT

We thank Mark Shearman and the medicinal chemistry department at Merck Sharp & Dohme for generously providing L-685,458, and several γ-secretase inhibitors before publication, Dirk Görlich for a plasmid encoding 2z-cDNA, and Armin Bosserhoff for radiosequencing of APP CTFs.

REFERENCES

1. Kang, J., Lemaire, H. G., Unterbeck, A., Salbaum, J. M., Masters, C. L., Grzeschik, K. H., Multhaup, G., Beyreuther, K., and Mueller-Hill, B. (1987) *Nature 325*, 733−736.
2. Jarrett, J. T., Berger, E. P., and Lansbury, P. T., Jr. (1993) *Biochemistry 32*, 4693−4697.
3. Selkoe, D. J. (1999) *Nature 399*, A23−31.
4. Wasco, W., Bupp, K., Magendantz, M., Gusella, J. F., Tanzi, R. E., and Solomon, F. (1992) *Proc. Natl. Acad. Sci. U.S.A. 89*, 10758−10762.
5. Wasco, W., Gurubhagavatula, S., Paradis, M. D., Romano, D. M., Sisodia, S. S., Hyman, B. T., Neve, R. L., and Tanzi, R. E. (1993) *Nat. Genet. 5*, 95−100.
6. Paliga, K., Peraus, G., Kreger, S., Dürrwang, U., Hesse, L., Multhaup, G., Masters, C. L., Beyreuther, K., and Weidemann, A. (1997) *Eur. J. Biochem. 250*, 354−363.
7. Weidemann, A., König, G., Bunke, D., Fischer, P., Salbaum, J. M., Masters, C. L., and Beyreuther, K. (1989) *Cell 57*, 115−126.
8. Haass, C., Schlossmacher, M. G., Hung, A. Y., Vigo Pelfrey, C., Mellon, A., Ostaszewski, B. L., Lieberburg, I., Koo, E. H., Schenk, D., Teplow, D. B., et al. (1992) *Nature 359*, 322−325.
9. Sinha, S., Anderson, J. P., Barbour, R., Basi, G. S., Caccavello, R., Davis, D., Doan, M., Dovey, H. F., Frigon, N., Hong, J., Jacobson-Croak, K., Jewett, N., Keim, P., Knops, J., Lieberburg, I., Power, M., Tan, H., Tatsuno, G., Tung, J., Schenk, D., Seubert, P., Suomensaari, S. M., Wang, S., Walker, D., John, V., et al. (1999) *Nature 402*, 537−540.
10. Vassar, R., Bennett, B. D., Babu-Khan, S., Kahn, S., Mendiaz, E. A., Denis, P., Teplow, D. B., Ross, S., Amarante, P., Loeloff, R., Luo, Y., Fisher, S., Fuller, J., Edenson, S., Lile, J., Jarosinski, M. A., Biere, A. L., Curran, E., Burgess, T., Louis, J. C., Collins, F., Treanor, J., Rogers, G., and Citron, M. (1999) *Science 286*, 735−741.
11. Yan, R., Bienkowski, M. J., Shuck, M. E., Miao, H., Tory, M. C., Pauley, A. M., Brashier, J. R., Stratman, N. C., Mathews, W. R., Buhl, A. E., Carter, D. B., Tomasselli, A. G., Parodi, L. A., Heinrikson, R. L., and Gurney, M. E. (1999) *Nature 402*, 533−537.
12. Gervais, F. G., Xu, D., Robertson, G. S., Vaillancourt, J. P., Zhu, Y., Huang, J., LeBlanc, A., Smith, D., Rigby, M., Shearman, M. S., Clarke, E. E., Zheng, H., Van Der Ploeg, L.

H., Ruffolo, S. C., Thornberry, N. A., Xanthoudakis, S., Zamboni, R. J., Roy, S., and Nicholson, D. W. (1999) *Cell 97*, 395−406.
13. LeBlanc, A., Liu, H., Goodyer, C., Bergeron, C., and Hammond, J. (1999) *J. Biol. Chem. 274*, 23426−23436.
14. Pellegrini, L., Passer, B. J., Tabaton, M., Ganjei, J. K., and D'Adamio, L. (1999) *J. Biol. Chem. 274*, 21011−21016.
15. Weidemann, A., Paliga, K., Dürrwang, U., Reinhard, F. B., Schuckert, O., Evin, G., and Masters, C. L. (1999) *J. Biol. Chem. 274*, 5823−5829.
16. Sherrington, R., Rogaev, E. I., Liang, Y., Rogaeva, E. A., Levesque, G., Ikeda, M., Chi, H., Lin, C., Li, G., Holman, K., Tsuda, T., Mar, L., Foncin, J.-F., Bruni, A. C., Montesi, M. P., Sorbi, S., Rainero, I., Pinessi, L., Nee, L., Chumakov, I., Pollen, D., Brookes, A., Sanseau, P., Polinsky, R. J., Wasco, W., Da Silva, H. A. R., Haines, J. L., Pericak-Vance, M. A., Tanzi, R. E., Roses, A. D., Fraser, P. E., Rommens, J. M., and St George-Hyslop, P. H. (1995) *Nature 375*, 754−760.
17. Levy-Lahad, E., Wasco, W., Pookaj, P., Romano, D., Oshima, J., Pettingell, P., Yu, C., Jondro, P. D., Schmidt, S. D., Wang, K., Crowley, A. C., Fu, Y.-H., Guenette, S. Y., Galas, D., Nemens, E., Wijsman, E. M., Bird, T. D., Schellenberg, G. D., and Tanzi, R. E. (1995) *Science 269*, 973−977.
18. Rogaev, E. I., Sherrington, R., Rogaeva, E. A., Levesque, G., Ikeda, M., Liang, Y., Chi, H., Lin, C., Holman, K., Tsuda, T., Mar, L., Sorbi, S., Nacmias, B., Piacentini, S., Amaducci, L., Chumakov, I., Cohen, D., Lannfelt, L., Fraser, P. E., Rommens, J. M., and Stgeorgehyslop, P. H. (1995) *Nature 376*, 775−778.
19. Scheuner, D., Eckman, C., Jensen, M., Song, X., Citron, M., Suzuki, N., Bird, T. D., Hardy, J., Hutton, M., Kukull, W., Larson, E., Levy-Lahad, E., Viitanen, M., Peskind, E., Poorkaj, P., Schellenberg, G., Tanzi, R., Wasco, W., Lannfelt, L., Selkoe, D., and Younkin, S. (1996) *Nat. Med. 2*, 864−870.
20. Duff, K., Eckman, C., Zehr, C., Yu, X., Prada, C. M., Pereztur, J., Hutton, M., Buee, L., Harigaya, Y., Yager, D., Morgan, D., Gordon, M. N., Holcomb, L., Refolo, L., Zenk, B., Hardy, J., and Younkin, S. (1996) *Nature 383*, 710−713.
21. Thinakaran, G., Borchelt, D. R., Lee, M. K., Slunt, H. H., Spitzer, L., Kim, G., Ratovitsky, T., Davenport, F., Nordstedt, C., Seeger, M., Hardy, J., Levey, A. I., Gandy, S. E., Jenkins, N. A., Copeland, N. G., Price, D. L., and Sisodia, S. S. (1996) *Neuron 17*, 181−190.
22. Citron, M., Westaway, D., Xia, W., Carlson, G., Diehl, T., Levesque, G., Johnson Wood, K., Lee, M., Seubert, P., Davis, A., Kholodenko, D., Motter, R., Sherrington, R., Perry, B., Yao, H., Strome, R., Lieberburg, I., Rommens, J., Kim, S., Schenk, D., Fraser, P., St George Hyslop, P., and Selkoe, D. J. (1997) *Nat. Med. 3*, 67−72.
23. Tomita, T., Maruyama, K., Saido, T. C., Kume, H., Shinozaki, K., Tokuhiro, S., Capell, A., Walter, J., Grunberg, J., Haass, C., Iwatsubo, T., and Obata, K. (1997) *Proc. Natl. Acad. Sci. U.S.A. 94*, 2025−2030.
24. Weidemann, A., Paliga, K., Dürrwang, U., Czech, C., Evin, G., Masters, C. L., and Beyreuther, K. (1997) *Nat. Med. 3*, 328−332.
25. Xia, W., Zhang, J., Perez, R., Koo, E. H., and Selkoe, D. J. (1997) *Proc. Natl. Acad. Sci. U.S.A. 94*, 8208−8213.
26. Pradier, L., Carpentier, N., Delalonde, L., Clavel, N., Bock, M. D., Buee, L., Mercken, L., Tocque, B., and Czech, C. (1999) *Neurobiol. Dis. 6*, 43−55.
27. Xia, W., Zhang, J., Ostaszewski, B. L., Kimberly, W. T., Seubert, P., Koo, E. H., and Selkoe, D. J. (1998) *Biochemistry 37*, 16465−16471.
28. Ray, W. J., Yao, M., Nowotny, P., Mumm, J., Zhang, W., Wu, J. Y., Kopan, R., and Goate, A. M. (1999) *Proc. Natl. Acad. Sci. U.S.A. 96*, 3263−3268.
29. De Strooper, B., Saftig, P., Craessaerts, K., Vanderstichele, H., Guhde, G., Annaert, W., Von Figura, K., and Van Leuven, F. (1998) *Nature 391*, 387−390.
30. Song, W., Nadeau, P., Yuan, M., Yang, X., Shen, J., and Yankner, B. A. (1999) *Proc. Natl. Acad. Sci. U.S.A. 96*, 6959−6963.
31. Wolfe, M. S., Xia, W., Ostaszewski, B. L., Diehl, T. S., Kimberly, W. T., and Selkoe, D. J. (1999) *Nature 398*, 513−517.
32. Lichtenthaler, S. F., Wang, R., Grimm, H., Uljon, S. N., Masters, C. L., and Beyreuther, K. (1999) *Proc. Natl. Acad. Sci. U.S.A. 96*, 3053−3058.
33. Higaki, J., Quon, D., Zhong, Z., and Cordell, B. (1995) *Neuron 14*, 651−659.
34. Murphy, M. P., Hickman, J., Eckman, C. B., Uljon, S. N., Wang, R., and Golde, T. E. (1999) *J. Biol. Chem. 274*, 11914−11923.
35. Simons, M., De Strooper, B., Multhaup, G., Tienari, P. J., Dotti, C. G., and Beyreuther, K. (1996) *J. Neurosci. 16*, 899−908.
36. Culvenor, J. G., Maher, F., Evin, G., Malchiodi Albedi, F., Cappai, R., Underwood, J. R., Davis, J. B., Karran, E. H., Roberts, G. W., Beyreuther, K., and Masters, C. L. (1997) *J. Neurosci. Res. 49*, 719−731.
37. Weidemann, A., Paliga, K., Dürrwang, U., Reinhard, F., Zhang, D., Sandbrink, R., Evin, G., Masters, C. L., and Beyreuther, K. (1999) in *Alzheimer's Disease: Methods and Protocols* (Hooper, N., Ed.) Methods in Molecular Medicine, Vol. 32, pp 333−344, Humana Press, Totowa, NJ.
38. Li, Y.-M., Xu, M., Lai, M.-T., Huang, Q., Castro, J. L., FiMunzio-Mower, J., Harrison, T., Lellis, C., Nadin, A., Neduvelli, J. G., Register, R. B., Sardan, M. K., Shearman, M. S., Smith, M. S., Smith, A. L., Shi, X.-P., Yin, K.-C., Shafer, J. A., and Gardell, S. J. (2000) *Nature 405*, 689−694.
39. Shearman, M. S., Beher, D., Clarke, E. E., Lewis, H. D., Harrison, T., Hunt, P., Nadin, A., Smith, A. L., Stevenson, G., and Castro, J. L. (2000) *Biochemistry 39*, 8698−8704.
40. Ida, N., Hartmann, T., Pantel, J., Schröder, J., Zerfass, R., Förstl, H., Sandbrink, R., Masters, C. L., and Beyreuther, K. (1996) *J. Biol. Chem. 271*, 22908−22914.
41. Schroeter, E. H., Kisslinger, J. A., and Kopan, R. (1998) *Nature 393*, 382−386.
42. Sisodia, S. S. (1992) *Proc. Natl. Acad. Sci. U.S.A. 89*, 6075−6079.
43. Parvathy, S., Hussain, I., Karran, E. H., Turner, A. J., and Hooper, N. M. (1999) *Biochemistry 38*, 9728−9734.
44. Lippincott-Schwartz, J., Yuan, L. C., Bonifacino, J. S., and Klausner, R. D. (1989) *Cell 56*, 801−813.
45. Citron, M., Diehl, T. S., Gordon, G., Biere, A. L., Seubert, P., and Selkoe, D. J. (1996) *Proc. Natl. Acad. Sci. U.S.A. 93*, 13170−13175.
46. Zhang, L., Song, L., and Parker, E. M. (1999) *J. Biol. Chem. 274*, 8966−8972.
47. De Strooper, B., Annaert, W., Cupers, P., Saftig, P., Craessaerts, K., Mumm, J. S., Schroeter, E. H., Schrijvers, V., Wolfe, M. S., Ray, W. J., Goate, A., and Kopan, R. (1999) *Nature 398*, 518−522.
48. McLendon, C., Xin, T., Ziani-Cherif, C., Murphy, M. P., Findlay, K. A., Lewis, P. A., Pinnix, I., Sambamurti, K., Wang, R., Fauq, A., and Golde, T. E. (2000) *FASEB J. 14*, 2383−2386.
49. Pinnix, I., Musunuru, U., Tun, H., Sridharan, A., Golde, T., Eckman, C., Ziani-Cherif, C., Onstead, L., and Sambamurti, K. (2001) *J. Biol. Chem. 276*, 481−487.
50. Tischer, E., and Cordell, B. (1996) *J. Biol. Chem. 271*, 21914−21919.
51. Gu, Y., Misonou, H., Sato, T., Dohmae, N., Takio, K., and Ihara, Y. (2001) *J. Biol. Chem. 276*, 35235−35238.
52. Yu, C., Kim, S. H., Ikeuchi, T., Xu, H., Gasparini, L., Wang, R., and Sisodia, S. S. (2001) *J. Biol. Chem. 276*, 43756−43760.
53. Sastre, M., Steiner, H., Fuchs, K., Capell, A., Multhaup, G., Condron, M. M., Teplow, D. B., and Haass, C. (2001) *EMBO Rep. 2*, 835−841.
54. Steiner, H., Duff, K., Capell, A., Romig, H., Grim, M. G., Lincoln, S., Hardy, J., Yu, X., Picciano, M., Fechteler, K., Citron, M., Kopan, R., Pesold, B., Keck, S., Baader, M., Tomita, T., Iwatsubo, T., Baumeister, R., and Haass, C. (1999) *J. Biol. Chem. 274*, 28669−28673.

55. Kimberly, W. T., Xia, W., Rahmati, T., Wolfe, M. S., and Selkoe, D. J. (2000) *J. Biol. Chem. 275*, 3173−3178.
56. Kuo, Y. M., Kokjohn, T. A., Watson, M. D., Woods, A. S., Cotter, R. J., Sue, L. I., Kalback, W. M., Emmerling, M. R., Beach, T. G., and Roher, A. E. (2000) *Am. J. Pathol. 156*, 797−805.
57. Ni, C. Y., Murphy, M. P., Golde, T. E., and Carpenter, G. (2001) *Science 294*, 2179−2181.
58. Sato, N., Urano, F., Yoon, D., Leem, J., Kim, S. H., Li, M., Donoviel, D., Bernstein, A., Lee, A. S., Ron, D., Veselits, M. L., Sisodia, S. S., and Thinakaran, G. (2000) *Nat. Cell Biol. 2*, 863−870.
59. Li, Y. M., Laim, M. T., Xum, M., Huangm, Q., DiMuzio-Mower, J., Sardana, M. K., Shi, X. P., Yin, K. C., Shafer, J. A., and Gardell, S. J. (2000) *Proc. Natl. Acad. Sci. U.S.A. 97*, 6138−6143.
60. Yu, G., Chen, F., Levesque, G., Nishimura, M., Zhang, D. M., Levesque, L., Rogaeva, E., Xu, D., Liang, Y., Duthie, M., St George-Hyslop, P. H., and Fraser, P. E. (1998) *J. Biol. Chem. 273*, 16470−16475.
61. Yu, G., Nishimura, M., Arawaka, S., Levitan, D., Zhang, L., Tandon, A., Song, Y. Q., Rogaeva, E., Chen, F., Kawarai, T., Supala, A., Levesque, L., Yu, H., Yang, D. S., Holmes, E., Milman, P., Liang, Y., Zhang, D. M., Xu, D. H., Sato, C., Rogaev, E., Smith, M., Janus, C., Zhang, Y., Aebersold, R., Farrer, L. S., Sorbi, S., Bruni, A., Fraser, P., and St George-Hyslop, P. H. (2000) *Nature 407*, 48−54.
62. Brown, M. S., Ye, J., Rawson, R. B., and Goldstein, J. L. (2000) *Cell 100*, 391−398.
63. Martys-Zage, J. L., Kim, S. H., Berechid, B., Bingham, S. J., Chu, S., Sklar, J., Nye, J., and Sisodia, S. S. (2000) *J. Mol. Neurosci. 15*, 189−204.
64. Minopoli, G., De Candia, P., Bonetti, A., Faraonio, R., Zambrano, N., and Russo, T. (2001) *J. Biol. Chem. 276*, 6545−6550.
65. Cao, X., and Südhof, T. C. (2001) *Science 293*, 115−120.
66. Petit, A., Bihel, F., Da Costa, C. A., Pourquie, O., Checler, F., and Kraus, J. L. (2001) *Nat. Cell Biol. 3*, 507−511.

BI015794O